CONFIDENTIAL

Copy No. 354
RM No. L8A28b

NACA

RESEARCH MEMORANDUM

DRAG MEASUREMENTS AT TRANSONIC SPEEDS OF TWO BODIES OF FINENESS RATIO 9 WITH DIFFERENT LOCATIONS OF MAXIMUM BODY DIAMETER

By

Jim Rogers Thompson and Max C. Kurbjun

Langley Memorial Aeronautical Laboratory
Langley Field, Va.

NATIONAL ADVISORY COMMITTEE FOR AERONAUTICS

WASHINGTON

July 22, 1948

CONFIDENTIAL

CONFIDENTIAL

ERRATA

NACA RM No. L8A28b

DRAG MEASUREMENTS AT TRANSONIC SPEEDS OF TWO BODIES OF FINENESS RATIO 9 WITH DIFFERENT LOCATIONS OF MAXIMUM BODY DIAMETER

By Jim Rogers Thompson and Max C. Kurbjun

July 22, 1948

Replace figures 7 and 8 with the attached revised figures.

CONFIDENTIAL

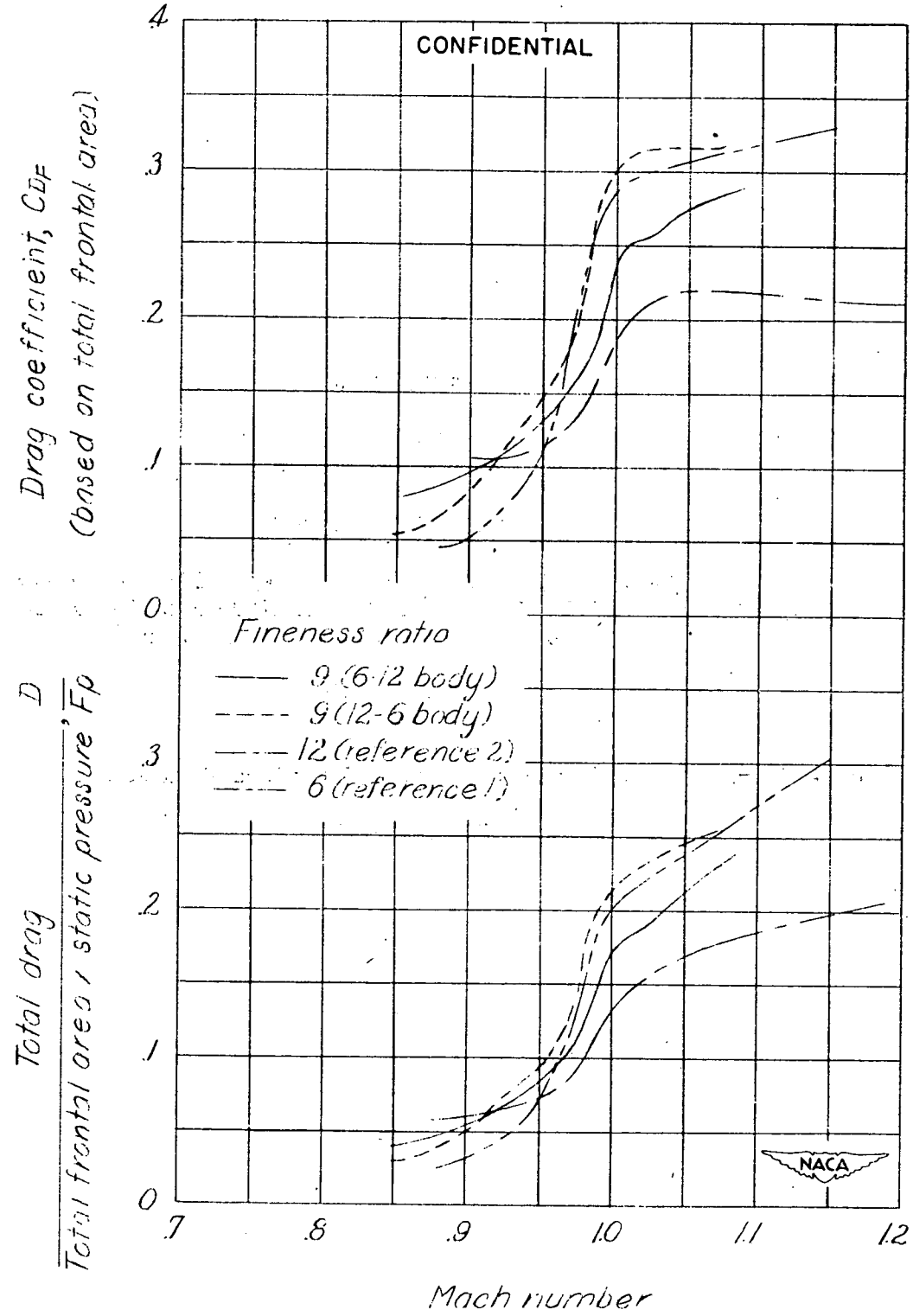

Figure 7.- Comparison of total drag results with those of previous tests.

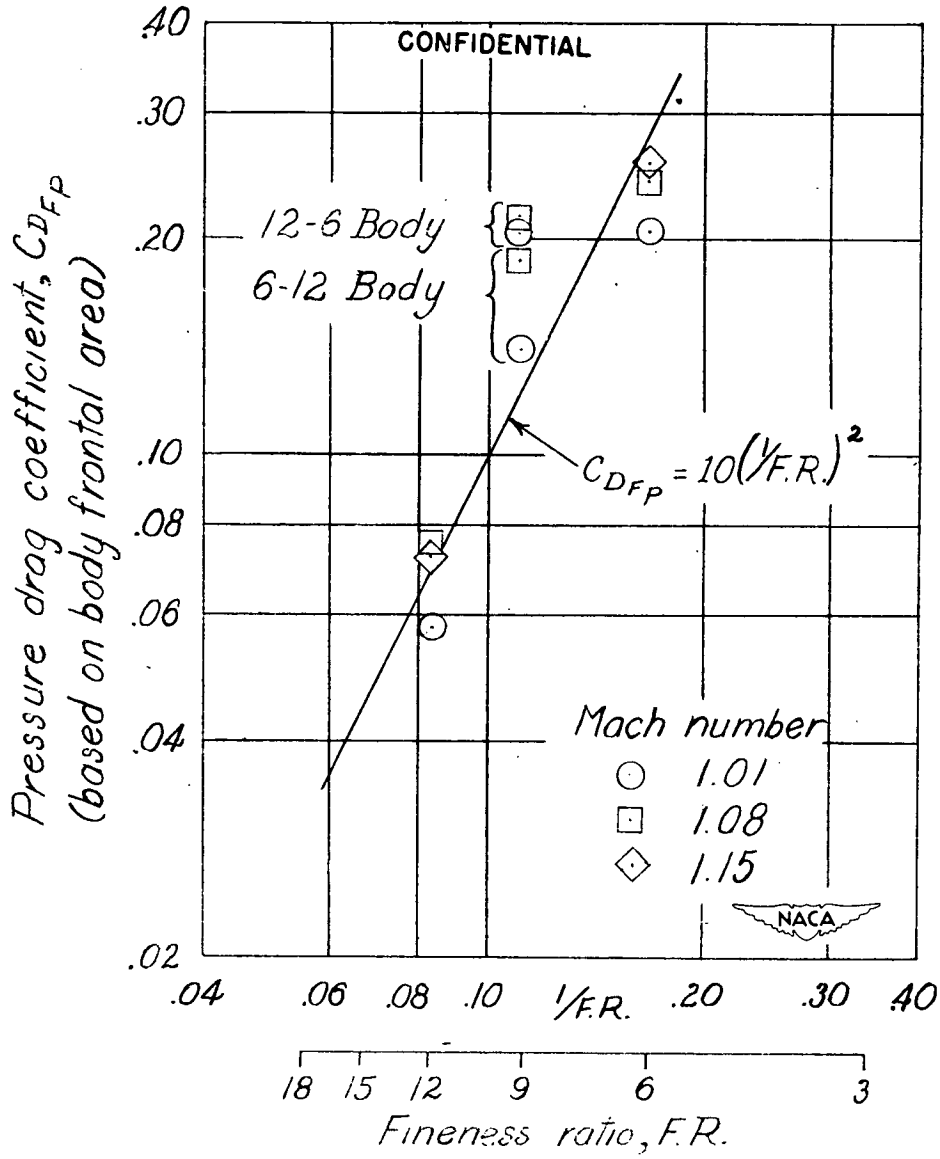

Figure 8.- Logarithmic variation of body pressure drag coefficients with fineness ratio for Mach numbers of 1.01, 1.08, and 1.15.

CONFIDENTIAL

NATIONAL ADVISORY COMMITTEE FOR AERONAUTICS

RESEARCH MEMORANDUM

DRAG MEASUREMENTS AT TRANSONIC SPEEDS OF TWO BODIES OF FINENESS RATIO 9 WITH DIFFERENT LOCATIONS OF MAXIMUM BODY DIAMETER

By Jim Rogers Thompson and Max C. Kurbjun

SUMMARY

As part of an investigation of the transonic drag characteristics of bodies of revolution, the drags of two bodies of fineness ratio 9 having maximum diameter locations 16.7 percent of the body length ahead of and behind the body midpoint have been measured by the free-fall method. The results obtained are compared with results which have been reported for similar bodies of fineness ratio 6 and 12 having the maximum diameter located at the body midpoint.

The body with the maximum diameter forward of the midpoint had 20 percent less drag at a Mach number of 1 and 10 percent less drag at a Mach number of 1.08 than did the body with the maximum diameter to the rear of the midpoint. The drag of both bodies was somewhat greater than that estimated for a similar body of fineness ratio 9 with the maximum diameter located at the midpoint.

The abrupt drag rise which occurs between Mach numbers of 0.95 and 1.0 is markedly affected by change of the shape of the body behind the maximum diameter and is relatively insensitive to large changes in the nose shape. This drag rise appears to result principally from the growth and rearward motion of the peak negative pressure on the body as the Mach number approaches unity. Further drag rise above Mach number 1 appears to be controlled principally by the nose shape.

INTRODUCTION

At transonic and low supersonic speeds, the fuselage contributes an undesirably large portion of the over-all drag of airplane configurations which utilize the low-drag capabilities of highly swept wings. In order to find means of reducing this fuselage drag, the Langley Laboratory of the National Advisory Committee for Aeronautics is investigating the drag characteristics of slender bodies of revolution (both with and without wings) at transonic and low supersonic speeds by use of free-fall, wing-flow, and rocket powered model techniques.

Results so far obtained by the free-fall method (references 1 and 2) have shown that increasing the fineness ratio from 6 to 12 considerably

reduced the body drag. The body shape used was derived from an NACA low-drag airfoil and had its maximum diameter located at the body midpoint. Some of the effects of swept wings on the drag of the fineness-ratio-12 body were reported in reference 3.

The present paper presents free-fall results showing the effect of the location of the maximum body diameter on the body drag. This test was initiated in order to provide information at high Reynolds number on the relative contributions of the front and rear sections of the body to the body drag without undertaking extensive pressure-distribution measurements.

APPARATUS AND METHOD

Test bodies.- Details and dimensions of the two test bodies are shown on the drawing (fig. 1), and photographs of the bodies are presented in figures 2 and 3. The test bodies were derived by combining the front half of a fineness-ratio-6 body (reference 1) and the rear half of a fineness-ratio-12 body (reference 2) and vice versa. The resulting fineness-ratio-9 bodies are herein referred to as the 6-12 body and 12-6 body, respectively. The location of the maximum thickness was 16.7 percent ahead of the body midpoint for the 6-12 body and 16.7 percent behind the body midpoint for the 12-6 body. The stabilizing tail assemblies of both bodies were identical with those of the bodies of fineness ratio 6 and 12.

Measurements.- Measurements of the desired quantities were accomplished as in previous tests (references 1 and 2) through use of the NACA radio-telemetering system and radar and phototheodolite equipment. The telemetering system was used to record the following quantities at two separate ground stations for each body:

1. The total drag as measured by a sensitive accelerometer alined with the longitudinal axis of the body

2. The total pressure at an orifice located at the nose of the body

3. The static pressure at two points located near the rear of the body (See fig. 1.)

A time history of the position of each body with respect to ground axes was recorded during its free fall by use of the radar and phototheodolite equipment. A survey of atmospheric pressure and temperature at various heights was obtained from synchronized altimeter, thermometer, radar, and phototheodolite readings taken during the descent of the airplane from which the bodies were dropped. The direction and speed of the horizontal components of the wind in the range of altitude for which data are presented were obtained from radar and phototheodolite records of the path of a free balloon.

Reduction of data.- As in previous tests, the velocity of each body with respect to the ground, referred to hereinafter as ground velocity, was obtained during its free fall both by differentiation of the flight path determined by the radar and phototheodolite equipment and by integration of the vector sums of gravitational acceleration and the directed retardation measured by the longitudinal accelerometer. The true airspeed was obtained by vector addition of the ground velocity and the horizontal wind velocity measured at the appropriate altitude.

The directly measured values of total drag D and velocity V were combined with the appropriate static pressure p, the temperature T, and the total frontal area F to obtain the variation of the nondimensional ratio D/Fp with the Mach number. Values of the conventional drag coefficient C_{D_F} based on frontal area were obtained from simultaneous values of D/Fp and Mach number by use of the relation

$$C_{D_F} = \frac{D/Fp}{\frac{\gamma}{2}M^2}$$

where the ratio of specific heats γ was taken as 1.4.

RESULTS

Time histories of the measured and computed quantities obtained for each test body are given in figures 4 and 5. Incomplete data were obtained for both bodies, in the case of the 6-12 body (fig. 4) due to structural failure of the stabilizing tail assembly after 41 seconds of free fall and in the case of the 12-6 body (fig. 5) due to complete failure of the telemetering equipment after 38 seconds of free fall. The tail failure is not believed due to flutter, as identical tails have been successfully used on other bodies (references 1 to 3) at speeds considerably above that at which the failure occurred. It is considered more probable that the failure resulted from a weakened or faulty glue joint in the wooden boom on which the tail surfaces were mounted. The telemetering equipment used for the pressure measurements operated intermittently in both cases and as a result these measurements are considered to be of insufficient accuracy to warrant detailed presentation. The measurements are cited, however, where large changes or definite trends were indicated.

The ground velocities obtained for the test bodies from the accelerometer data are shown in figures 4 and 5 as dashed lines and those from the radar and phototheodolite equipment by test points. The radar and phototheodolite test points are evenly distributed about the accelerometer data but contain a scatter somewhat greater than usual for this equipment. This scatter resulted from partial failure of the theodolite photographic equipment during the test, necessitating the use of a less precise auxiliary recording device. The Mach numbers computed from the true airspeed (shown in the time histories as solid lines) are believed accurate

within ±0.01. Mach numbers determined from the telemetered total pressure (when obtained) and the static pressure from the pressure-temperature survey agreed with the Mach numbers determined from the true airspeed-temperature data within ±0.03.

The agreement between the ground velocities obtained from the radar and phototheodolite data and from the accelerometer data (see figs. 4 and 5) indicates that the maximum possible uncertainty in the acceleration measurement is of the order of ±0.01g. The corresponding uncertainty in D/Fp is ±0.008 at a Mach number of 0.85 and decreases as the drag and static pressure increase during the free fall to ±0.004 at a Mach number of 1.08. The values of C_{D_F} are somewhat less accurate due to the uncertainty in Mach number of ±0.01. The total uncertainty in C_{D_F} is ±0.020 at M = 0.85 and ±0.012 at M = 1.08.

Curves are presented in figure 6 showing the variation with Mach number of D/Fp and C_{D_F} for the 6-12 and 12-6 bodies. As the drag of the small stabilizing tail surfaces was not separately measured, the drag parameters shown in figure 6 were computed from the total drags and frontal areas.

Examination of figure 6 shows that the total drag of the 6-12 body increased abruptly from 0.10 of atmospheric pressure per unit of frontal area at a Mach number of 0.97 to 0.17 at 1.00 and then increased less rapidly to 0.24 at 1.08. The total drag of the 12-6 body increased abruptly from 0.10 of atmospheric pressure per unit of frontal area at a Mach number of 0.96 to 0.21 at 1.00 and attained a value of 0.26 at 1.08. The 6-12 body had 20 percent less drag than the 12-6 body at the speed of sound and 10 percent less drag at a Mach number of 1.08.

DISCUSSION

The results obtained for the 6-12 and 12-6 bodies are compared in figure 7 with results for the bodies of fineness ratio 6 and 12 (references 1 and 2) from which they were derived. Inspection of figure 7 shows that in the region where the abrupt drag rise occurs (Mach numbers of 0.95 to 1.00) the drag variation for the 12-6 body is similar to that of the fineness-ratio-6 body and that of the 6-12 body is similar to that of the fineness-ratio-12 body. Thus, in this region, the shape of the body behind the maximum diameter appears to be the controlling influence on the drag. This observation is consistent with the results of reference 4 which presents pressure-distribution measurements at transonic speeds by the NACA wing-flow method on a circular-arc body of fineness ratio 6. Reference 4 shows that the abrupt drag rise occurred mainly on the rear portion of the body as a growth and rearward motion of the peak negative pressure as the Mach number approached unity.

The pressure measurements obtained near M = 1 in the present test are also consistent with the results of reference 4 as they showed an abrupt drop from a positive value to a negative value of the pressure coefficient at the orifice at X = 81 inches (90 percent of the body length) on the 12-6 body and a much smaller drop from a positive value to a smaller positive value at the orifice at X = 72 inches (80 percent of the body length) on the 6-12 body. The locations of these orifices are shown in figure 1. Although these pressure variations could also have resulted from separation occurring at some point ahead of the orifices, it is not considered likely as no appreciable separation was observed in the tests of reference 4. The Reynolds number (based on the body length) varied from 0.8 to 1.6×10^6 for the tests of reference 4 and increased from 18×10^6 at a Mach number of 0.85 to 37×10^6 at a Mach number of 1.08 for the present tests.

At Mach numbers greater than 1.0, figure 7 shows that the curve for the 12-6 body tends to follow that of the fineness-ratio-12 body and that of the 6-12 body tends to follow that of the fineness-ratio-6 body. Here, the nose of the body appears to be the factor which controls the rate of drag increase.

On the basis of these data, the drag rise apparently occurs as follows: the initial steep rise between Mach numbers of 0.95 and 1.0 results from a growth and rearward motion of the peak negative pressure on the body and is relatively insensitive to nose shape, while the controlling influence in any further drag rise appears to be the nose shape.

Figure 8 shows approximate values of the body pressure drag coefficients corresponding to the data of figure 7 at several low supersonic Mach numbers. These values were obtained by subtracting the tail drag and the estimated body skin-friction drag from the measured total drag. The body skin-friction coefficient was assumed to be 0.003 based on surface area. Inasmuch as the tail drags for the bodies of fineness ratio 9 and 12 were not measured, values of tail drag were estimated by averaging the tail drag results for the fineness-ratio-6 body (reference 1) and results for an identical tail mounted on a fineness-ratio-12 body fitted with a sweptback wing (reference 3). The differences between the two separate measurements of tail drag correspond to a very small part of the total drag at the low supersonic Mach numbers considered and do not significantly affect the results presented here. Variations with fineness ratio of the body pressure drag coefficients obtained in this manner are shown plotted to logarithmic scales in figure 8 for Mach numbers of 1.01, 1.08, and 1.15. The data for the bodies of fineness ratio 6 and 12 are fitted closely by a line of slope 2 indicating that the variation of the pressure drag coefficient with fineness ratio may be represented by the equation

$$C_{D_{FP}} = K\left(\frac{1}{F.R.}\right)^2$$

with K being approximately equal to 10. Lighthill, in reference 5, derived the same relation from the linearized supersonic potential-flow equations and, in addition, found that the minimum theoretically possible value of K was π^2 . (9.87). This value, however, corresponded to a blunt-ended body which was not admissible within his assumptions. Reference 5 recommends a parabolic body shape (K = 10.67) as being the optimum "practical" body. The results from the linearized theory should not apply in the case of the bodies used herein, however, due to the bluntness of the nose shape which would result in a region of subsonic flow of unknown extent at the Mach numbers considered. The result obtained is analogous to that presented in reference 6 which shows that for relatively thick round nosed airfoils the pressure drag coefficient is proportional to the square of the airfoil thickness ratio in the range of Mach numbers therein investigated (1.0 to 1.15).

The points corresponding to the 6-12 and 12-6 bodies in figure 8 lie above the line of slope 2 through the points for the bodies of fineness ratio 6 and 12. This indicates that in the Mach number range from 1.01 to 1.08 location of the maximum body diameter either 16.7 percent of the body length ahead (6-12) or behind (12-6) the midpoint of the body resulted in a higher pressure drag than the value estimated for a fineness-ratio-9 body of this family with the maximum diameter located at the midpoint. Location of the maximum diameter ahead of the midpoint did not increase the drag as much as location of the maximum diameter behind the midpoint; however, it is apparent from figure 6 that the curves tend to converge somewhat beyond the explored Mach number range.

CONCLUDING REMARKS

Measurements of the total drag of two bodies of fineness ratio 9 having maximum diameter locations 16.7 percent of the body length ahead (6-12) and behind (12-6) the midpoint of the body have been made by the free-fall method.

The results showed that the 6-12 body had about 20 percent less drag at a Mach number of 1 than the 12-6 body; however, at a Mach number of 1.08 the difference had decreased to 10 percent. The drag of both bodies was somewhat higher at low supersonic speeds than that estimated for a similar body of fineness ratio 9 with the maximum diameter located at the midpoint.

The abrupt drag rise which occurs between Mach numbers of 0.95 and 1.00 is markedly affected by change of the shape of the body behind the maximum diameter and is relatively insensitive to large changes in the nose shape. This drag rise appears to result principally from the growth and rearward motion of the peak negative pressure on the body as

the Mach number approaches unity. Further drag rise above Mach number 1 appears to be principally controlled by the nose shape.

Langley Memorial Aeronautical Laboratory
National Advisory Committee for Aeronautics
Langley Field, Va.

REFERENCES

1. Bailey, F. J., Jr., Mathews, Charles W., and Thompson, Jim Rogers: Drag Measurements at Transonic Speeds on a Freely Falling Body. NACA ACR No. L5E03, 1945.

2. Thompson, Jim Rogers, and Mathews, Charles W.: Total Drag of a Body of Fineness Ratio 12 and Its Stabilizing Tail Surfaces Measured during Free Fall at Transonic Speeds. NACA CB No. L6D08, 1946.

3. Mathews, Charles W., and Thompson, Jim Rogers: Comparison of the Transonic Drag Characteristics of Two Wing-Body Combinations Differing Only in the Location of the 45° Sweptback Wing. NACA RM No. L7I01, 1947.

4. Danforth, Edward C. B., and Johnston, J. Ford: Pressure Distribution over a Sharp-Nose Body of Revolution at Transonic Speeds by the NACA Wing-Flow Method. NACA RM No. L7K12, 1948.

5. Lighthill, M. J.: Supersonic Flow past Bodies of Revolution. R. & M. No. 2003, British A.R.C., 1945.

6. Thompson, Jim Rogers, and Mathews, Charles W.: Measurements of the Effects of Thickness Ratio and Aspect Ratio on the Drag of Rectangular-Plan-Form Airfoils at Transonic Speeds. NACA RM No. L7E08, 1947.

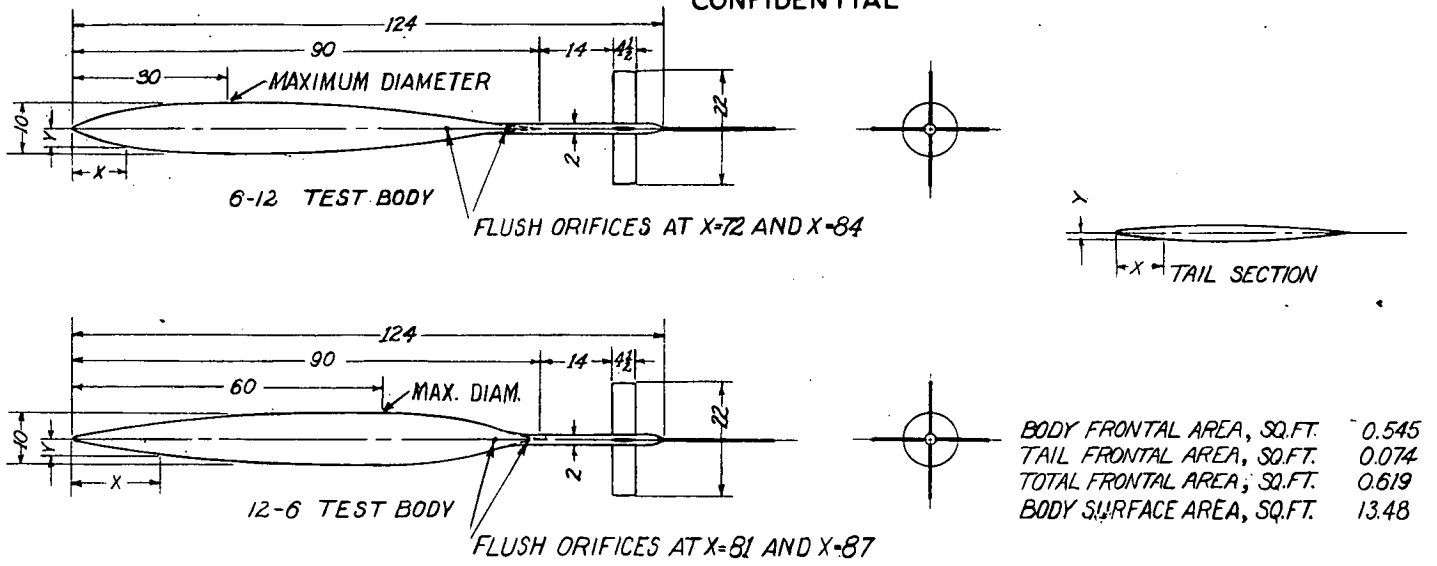

BODY FRONTAL AREA, SQ.FT.	0.545
TAIL FRONTAL AREA, SQ.FT.	0.074
TOTAL FRONTAL AREA, SQ.FT.	0.619
BODY SURFACE AREA, SQ.FT.	13.48

BODY COORDINATES, IN.
12-6 TEST BODY

X	Y	X	Y
0.00	0.000	48.00	4.876
.60	.277	54.00	4.971
.90	.358	60.00	5.000
1.50	.514	63.00	4.955
3.00	.866	66.00	4.828
6.00	1.446	69.00	4.610
9.00	1.936	72.00	4.274
12.00	2.365	75.00	3.754
18.00	3.112	78.00	3.031
24.00	3.708	81.00	2.222
30.00	4.158	84.00	1.350
36.00	4.489	87.00	.526
42.00	4.719	90.00	.000
NOSE RADIUS: 0.060			

BODY COORDINATES, IN.
6-12 TEST BODY

X	Y	X	Y
0.00	0.000	24.00	4.876
.30	.277	27.00	4.971
.45	.358	30.00	5.000
.75	.514	36.00	4.955
1.50	.866	42.00	4.828
3.00	1.446	48.00	4.610
4.50	1.936	54.00	4.274
6.00	2.365	60.00	3.754
9.00	3.112	66.00	3.031
12.00	3.708	72.00	2.222
15.00	4.158	78.00	1.350
18.00	4.489	84.00	.526
21.00	4.719	90.00	.000
NOSE RADIUS: 0.060			

TAIL-SECTION COORDINATES, IN.
NACA 16-SERIES AIRFOIL

X	Y	X	Y
0.000	0.000	1.350	0.122
.052	.029	1.800	.132
.113	.041	2.250	.135
.225	.056	2.700	.131
.338	.068	3.150	.118
.450	.078	3.600	.094
.675	.093	4.050	.057
.900	.105	4.275	.032
1.125	.115	4.500	.003
L.E. RADIUS: 0.008			

NACA

CONFIDENTIAL

Figure 1.- Details and dimensions of the test configurations. All dimensions are in inches.

NACA RM No. L8A28b

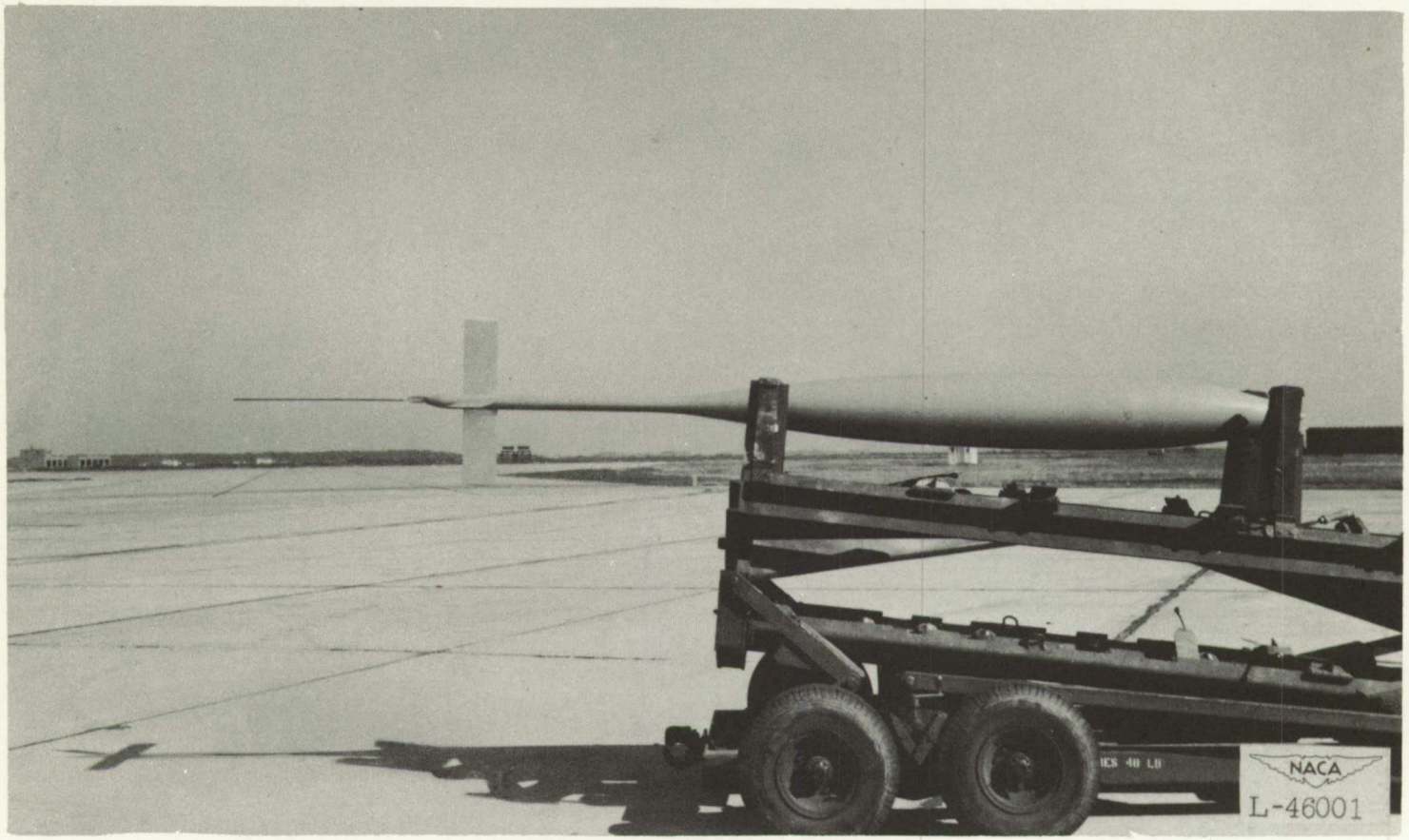

Figure 2.- Side view of the 6-12 test body.

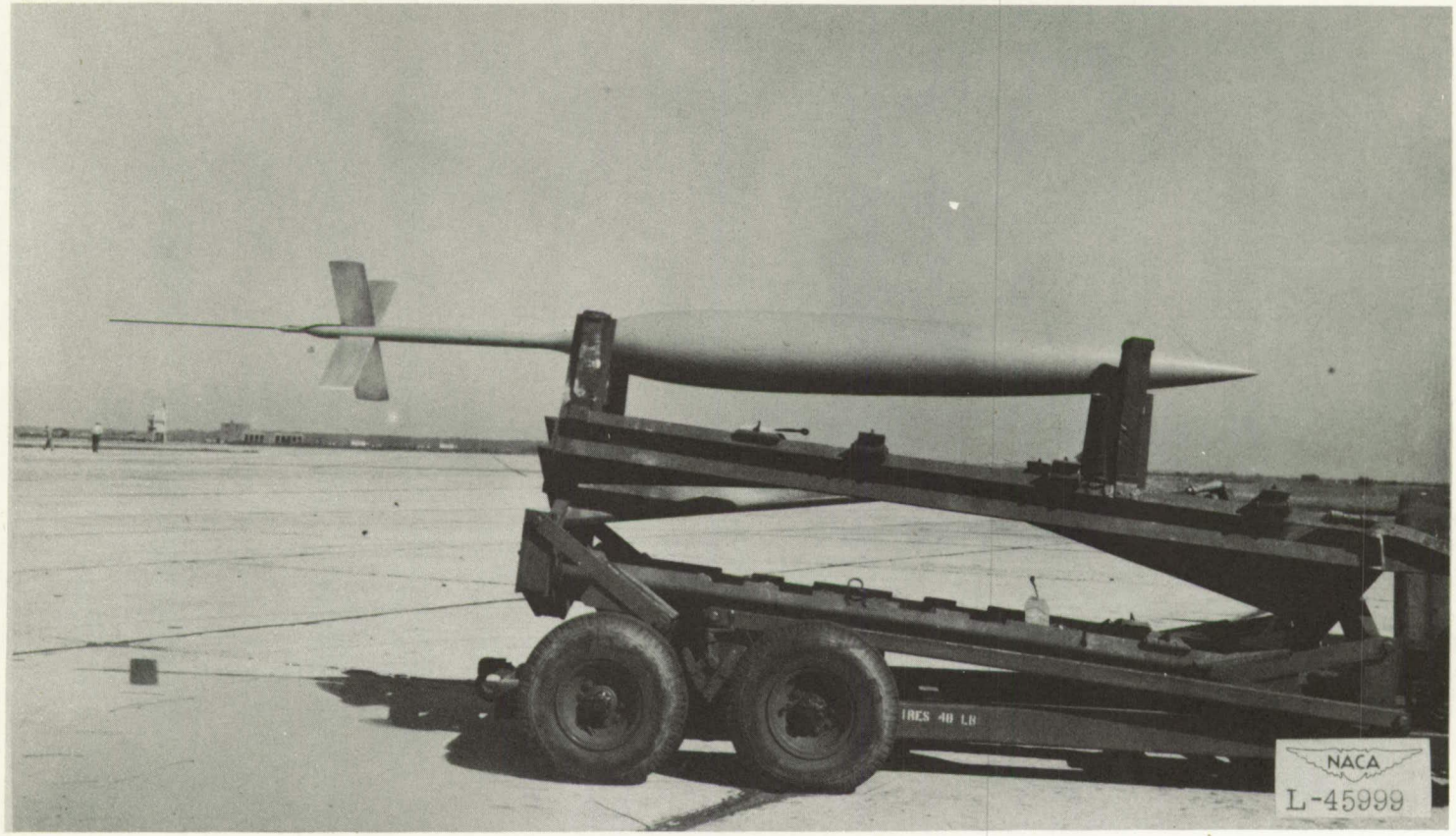

Figure 3.- Side view of the 12-6 test body.

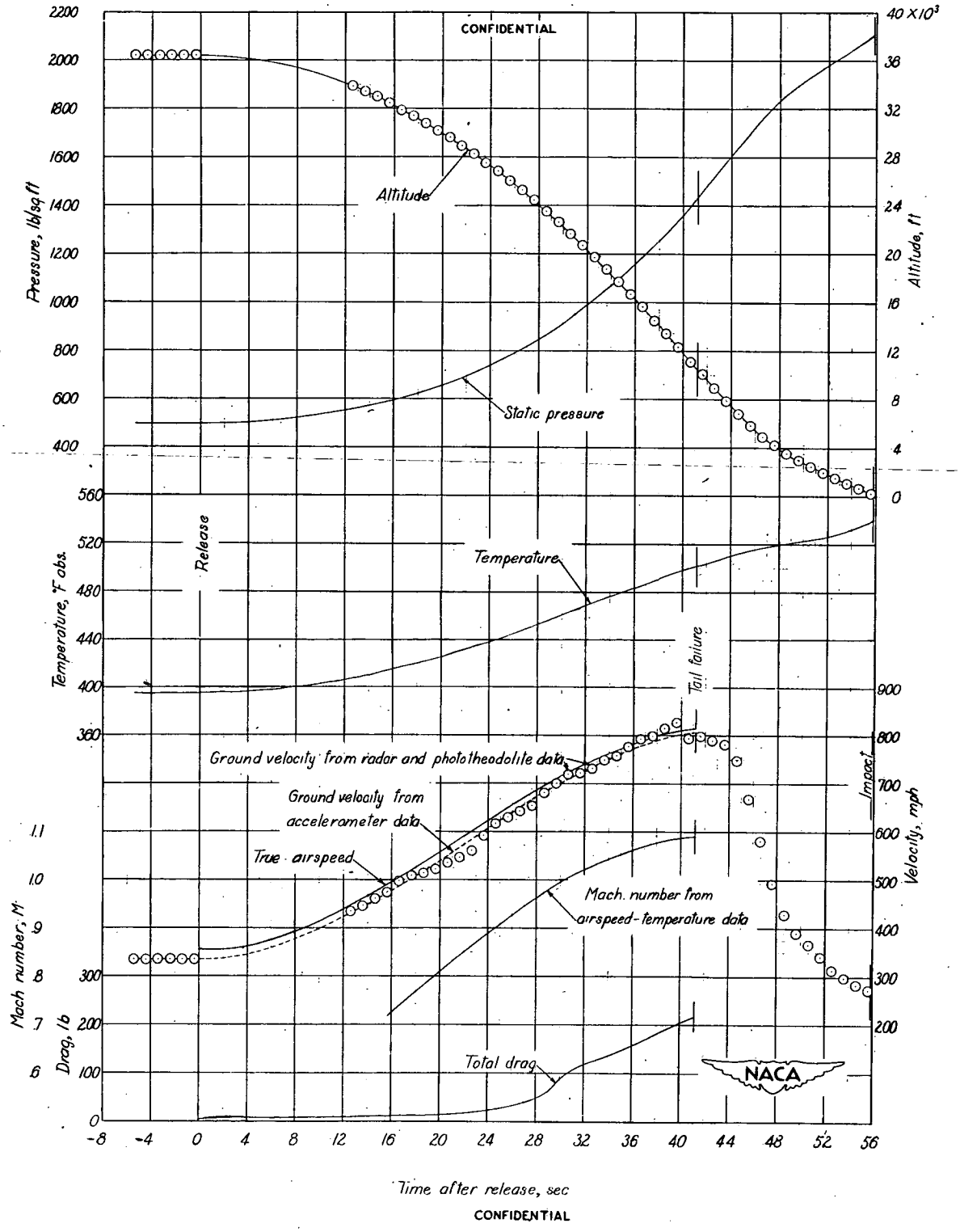

Figure 4.- Time history of free fall of the 6-12 test body.

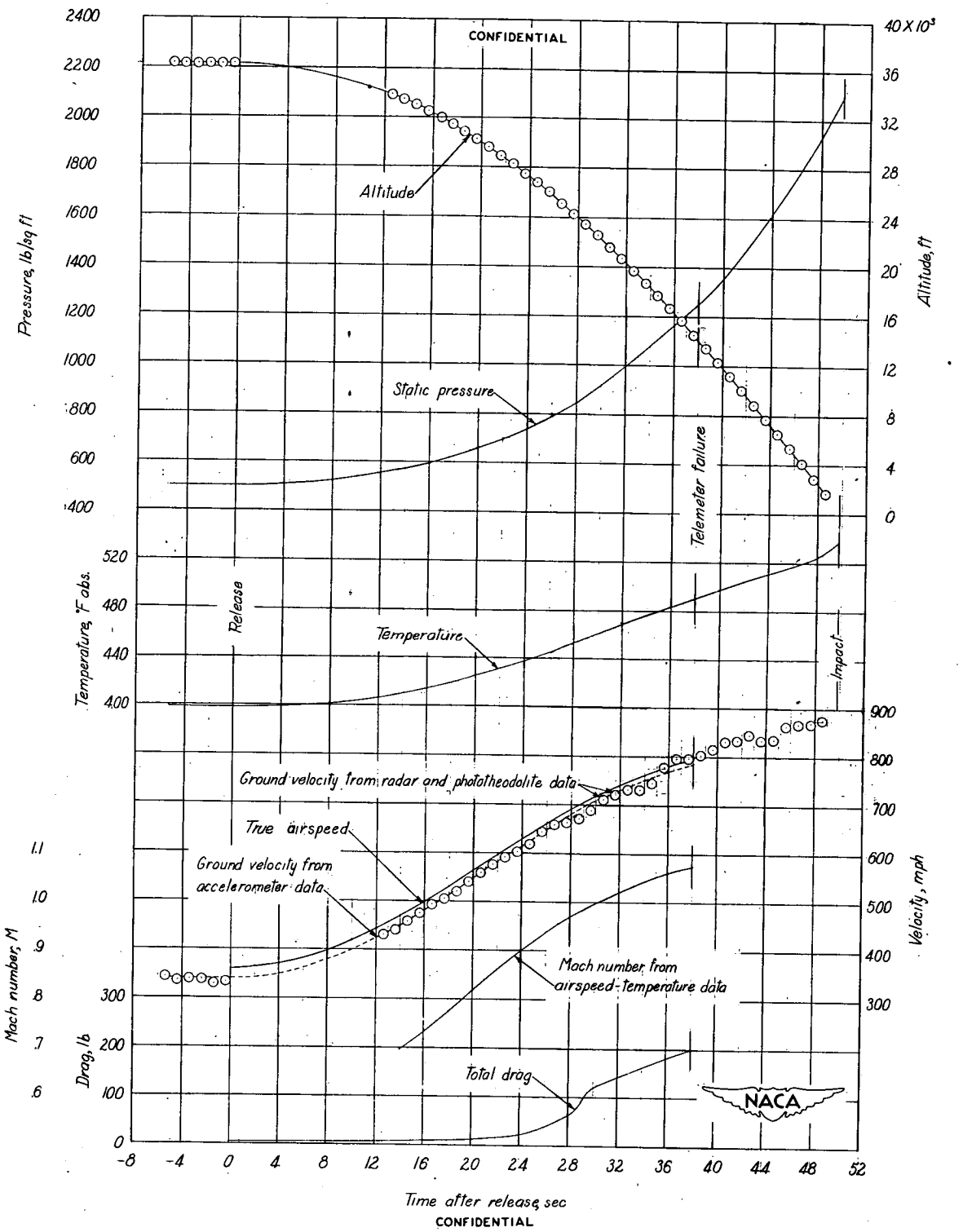

Figure 5.- Time history of free fall of the 12-6 test body.

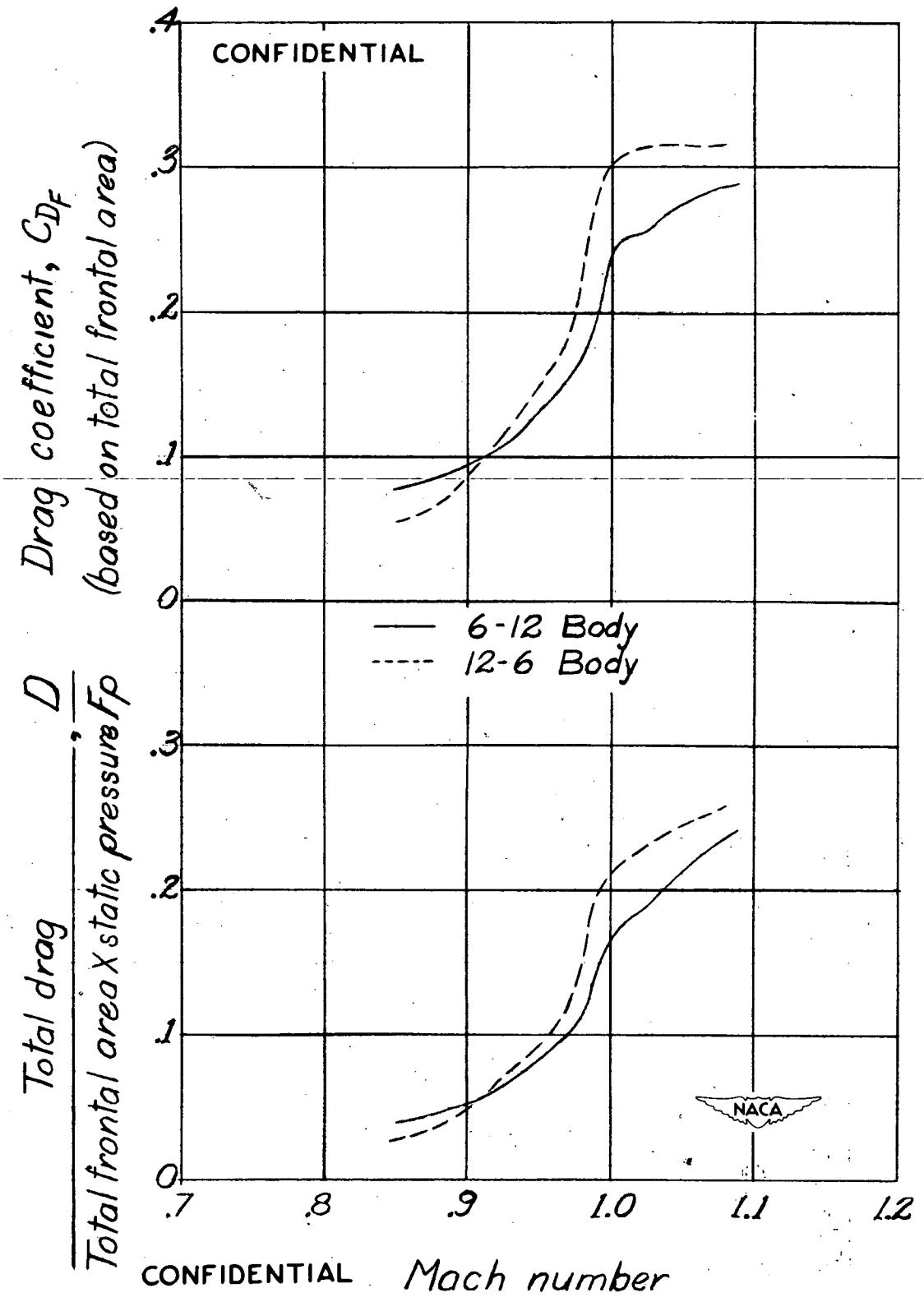

Figure 6.- Variation of C_{D_F} and D/F_p with Mach number for the 6-12 and 12-6 test bodies.

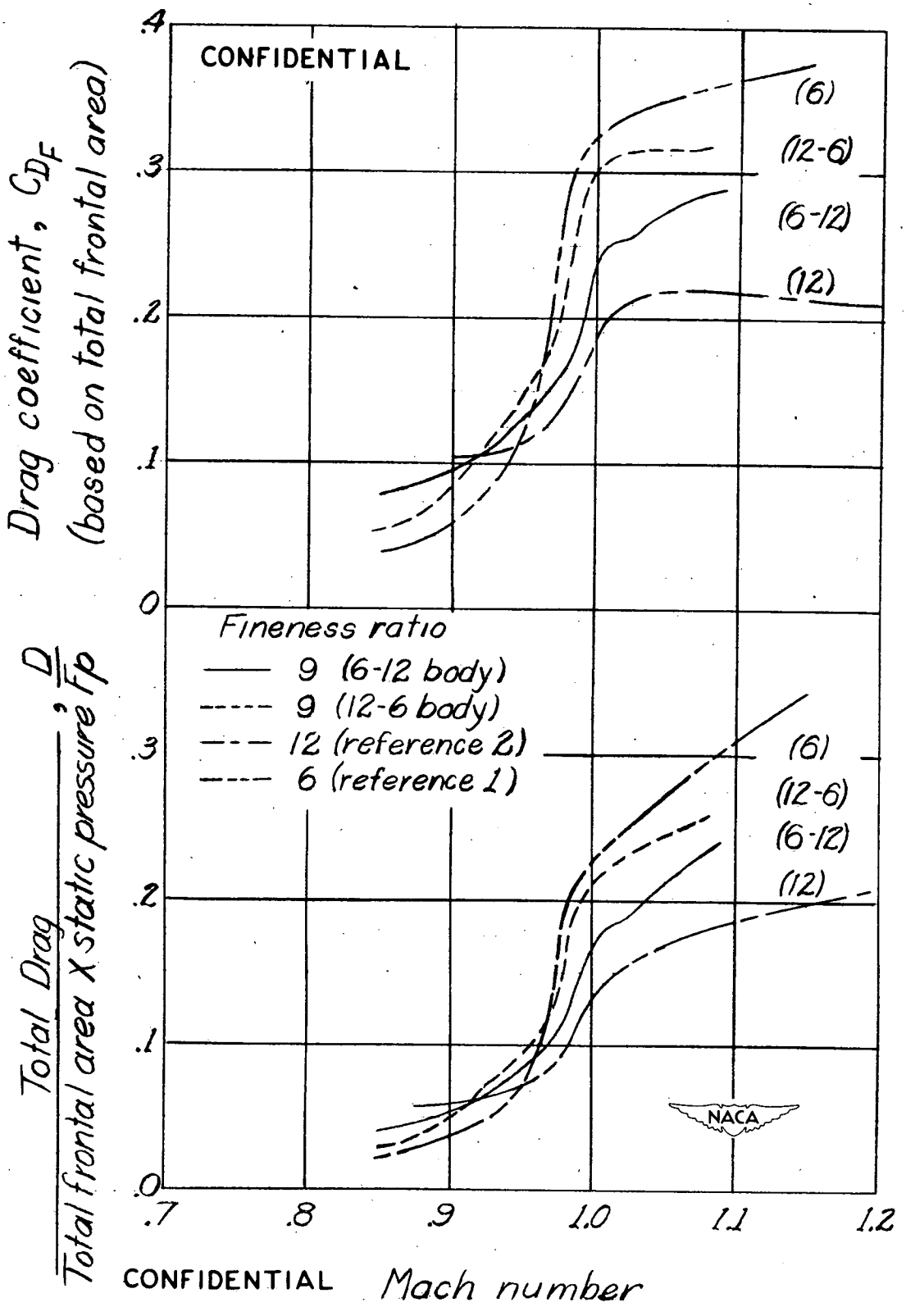

Figure 7.- Comparison of total drag results with those of previous tests.

NACA RM No. L8A28b

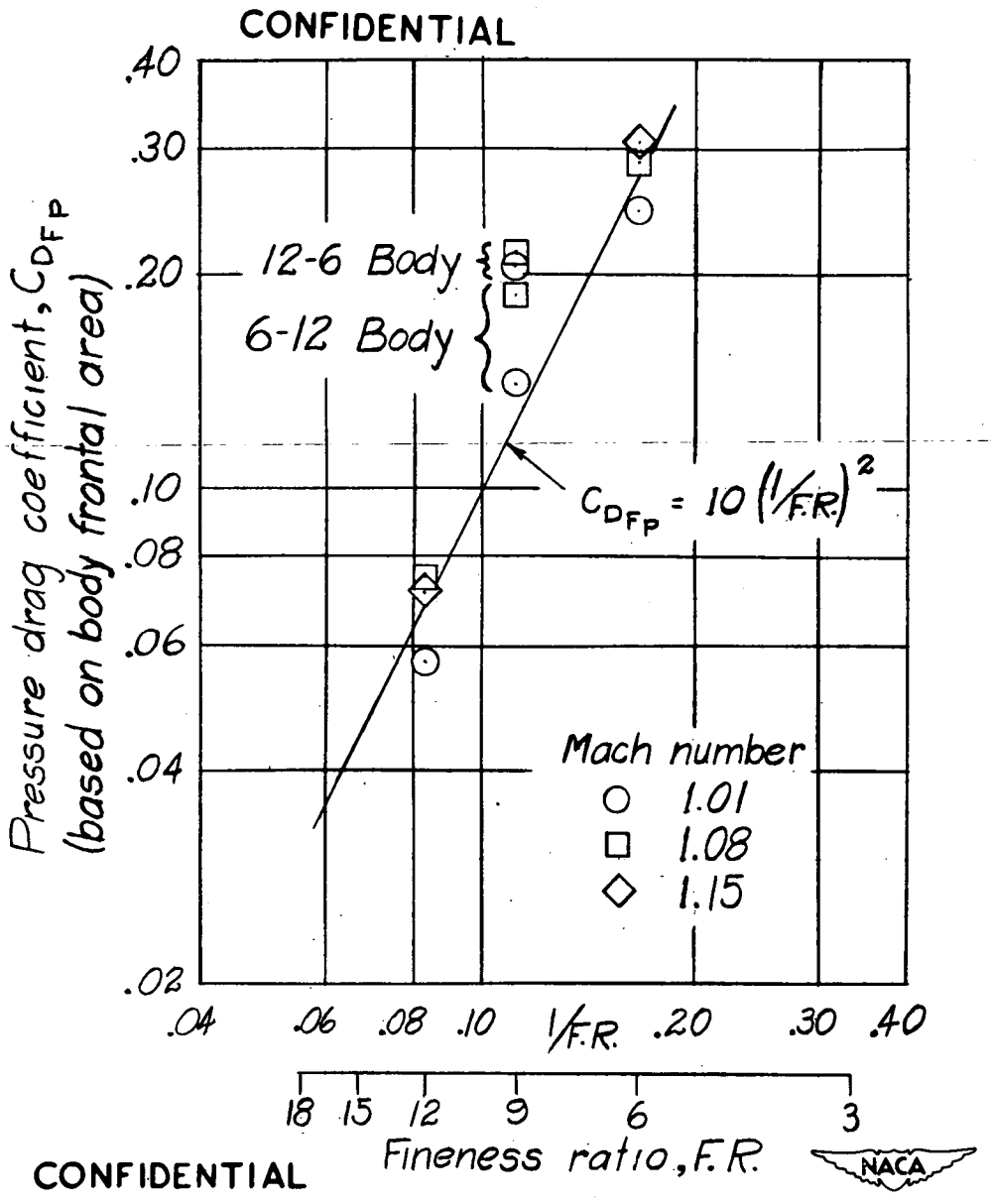

Figure 8.- Logarithmic variation of body pressure drag coefficients with fineness ratio for Mach numbers of 1.01, 1.08, and 1.15.